

Weak interaction corrections to muon pair production via the photon fusion at the LHC

S. I. Godunov^{1,*}, E. K. Karkaryan¹, V. A. Novikov¹, A. N. Rozanov², M. I. Vysotsky¹ and E. V. Zhemchugov¹

¹*E. Tamm Department of Theoretical Physics, Lebedev Physical Institute, 53 Leninskiy Prospekt, Moscow, 119991, Russia*

²*Centre de Physique de Particules de Marseille (CPPM), Aix-Marseille Universite, CNRS/IN2P3, 163 avenue de Luminy, case 902, Marseille, 13288, France*



(Received 24 August 2023; accepted 23 October 2023; published 20 November 2023)

Analytical formulas describing the correction due to the Z boson exchange to the cross section of the reaction $pp \rightarrow p\mu^+\mu^-X$ are presented. When the invariant mass of the produced muon pair $W \gtrsim 150$ GeV and its total transverse momentum is large, the correction is of the order of 20%.

DOI: [10.1103/PhysRevD.108.093006](https://doi.org/10.1103/PhysRevD.108.093006)

I. INTRODUCTION

The ATLAS collaboration measured the cross section of muon pair production in ultraperipheral collisions (UPCs) of protons at the Large Hadron Collider [1]. In the case of UPCs the lepton pair is produced in the $\gamma\gamma$ fusion and is accompanied by forward scattering of both protons. We calculated the corresponding cross section in [2]. Our result agrees with the one obtained by the ATLAS collaboration within the experimental accuracy. The results obtained with the help of Monte Carlo simulations can be found in [3–6]. The $\mu^+\mu^-$ pair production occurs in γZ and ZZ fusion as well. However, for the scattered proton to remain intact the square of the 4-momentum of the emitted photon (or Z boson) Q^2 should not considerably exceed $(200 \text{ MeV})^2$, since for larger Q^2 the cross section is suppressed by the elastic form factor ([7] Appendix A). Thus the contribution of the diagram with the virtual Z boson exchange is suppressed by the factor $Q^2/M_Z^2 \sim 10^{-5}$ and can be safely omitted. But if only one of the protons remains intact while the second one dissolves producing a hadron jet then substitution of the photon emitted by the second proton by a Z boson may lead to numerically noticeable corrections. This is so since the value of Q^2 is now bounded from above only by the invariant mass of the produced muon pair W (for $Q^2 > W^2$ the cross section of muon pair production is suppressed as a power of W^2/Q^2). In this way the contribution from the Z boson exchange being

proportional to $[Q^2/(M_Z^2 + Q^2)]^2$ can become noticeable for $W^2 \gtrsim M_Z^2$. Both the CMS and the ATLAS collaborations reported [8,9] observation of the reaction of lepton pair (e^+e^- or $\mu^+\mu^-$) production when one of the scattered protons is detected by forward detector (the CMS-TOTEM precision proton spectrometer or the ATLAS Forward Proton Spectrometer). The other proton can remain intact or disintegrate. In the latter case in [9] the events were selected in which the momentum squared of the emitted photon did not exceed $(5 \text{ GeV})^2$ (see our recent paper [10] with formulas and numerical estimates of the cross sections measured in [9]).

Dilepton production in proton-proton collisions through $\gamma\gamma$ fusion with the first proton scattered elastically while the second one produced a hadron jet was considered in our paper [11]. Analytical formulas describing the cross section of a muon pair production were derived therein. In the present paper we calculate weak interaction corrections to the cross section obtained in [11], which should be used for comparison of the Standard Model predictions with future experimental data. New physics can manifest itself in interactions of muons at high energies. Thus accurate Standard Model predictions are needed to probe it. Tiny deviations of the measured value of muon magnetic moment from the Standard Model result [12,13] may indicate considerable deviation of muon pair production cross section at large invariant masses of muon pair $W \sim 100 \text{ GeV} \div 1 \text{ TeV}$. To find them the results of the present paper should be accounted for.

Reactions of lepton pair production with $Z^*(Z^*Z^*)$ in the initial state were considered in [14] in the structure function approach.

In Sec. II general formulas are derived. Z boson exchange contributions are discussed in Sec. III. Numerical results are presented in Sec. IV and in Sec. V we conclude.

*Corresponding author: sigodunov@lebedev.ru

Published by the American Physical Society under the terms of the [Creative Commons Attribution 4.0 International license](https://creativecommons.org/licenses/by/4.0/). Further distribution of this work must maintain attribution to the author(s) and the published article's title, journal citation, and DOI. Funded by SCOAP³.

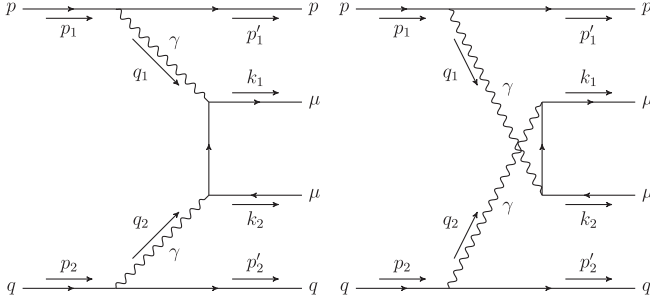


FIG. 1. Muon pair production in the photon fusion. The photon with momentum q_1 is radiated by the elastically scattered proton and the photon with momentum q_2 is radiated by the quark.

II. MUON PAIR PRODUCTION IN $\gamma\gamma$ FUSION

Diagrams for muon pair production in ultraperipheral collisions of protons are shown in Fig. 1.

The cross section for two-photon production can be expressed in terms of the amplitude $M_{\mu\alpha}$ of $\gamma\gamma \rightarrow \mu^+\mu^-$ transition as follows (see [10] and the review of two-photon particle production [15]):

$$\begin{aligned} d\sigma_{pq \rightarrow p\mu^+\mu^-q} &= 2 \cdot \frac{Q_q^2 (4\pi\alpha)^2}{(q_1^2)^2 (q_2^2)^2} (q_1^2 \rho_{\mu\nu}^{(1)}) (q_2^2 \rho_{\alpha\beta}^{(2)}) M_{\mu\alpha} M_{\nu\beta}^* \\ &\times \frac{(2\pi)^4 \delta^{(4)}(q_1 + q_2 - k_1 - k_2) d\Gamma}{4\sqrt{(p_1 p_2)^2 - m_p^4}} \\ &\times \frac{d^3 p'_1}{(2\pi)^3 2E'_1} \frac{d^3 p'_2}{(2\pi)^3 2E'_2} f_q(x, Q_2^2) dx, \end{aligned} \quad (1)$$

where the leading factor of 2 takes into account the symmetrical process where the other proton survives, α is the fine structure constant, Q_q is the charge of quark q , $\rho_{\mu\nu}^{(1)}$ and $\rho_{\mu\nu}^{(2)}$ are the density matrices of the photons, $d\Gamma$ is the phase space of the muon pair, m_p is the proton mass, $f_q(x, Q_2^2)$ is the parton distribution function (PDF) for

quark q , x is the fraction of the momentum of the disintegrating proton carried by the quark, $Q_2^2 = -q_2^2$, E'_1 and E'_2 are the energies of the proton and the quark after the collision.

For the density matrix $\rho^{(1)}$ originating from the elastically scattered proton we have [see Eqs. (25)–(27) from [10]]:

$$\begin{aligned} \rho_{\mu\nu}^{(1)} &= -\left(g_{\mu\nu} - \frac{q_{1\mu} q_{1\nu}}{q_1^2}\right) G_M^2(Q_1^2) \\ &\quad - \frac{(2p_1 - q_1)_\mu (2p_1 - q_1)_\nu}{q_1^2} D(Q_1^2), \\ D(Q_1^2) &= \frac{G_E^2(Q_1^2) + (Q_1^2/4m_p^2) G_M^2(Q_1^2)}{1 + Q_1^2/4m_p^2}. \end{aligned} \quad (2)$$

Here $Q_1^2 = -q_1^2$, and $G_E(Q_1^2)$, $G_M(Q_1^2)$ are the Sachs form factors of the proton. For the latter we use the dipole approximation:

$$\begin{aligned} G_E(Q^2) &= \frac{1}{(1 + Q^2/\Lambda^2)^2}, \quad G_M(Q^2) = \frac{\mu_p}{(1 + Q^2/\Lambda^2)^2}, \\ \Lambda^2 &= \frac{12}{r_p^2} = 0.66 \text{ GeV}^2, \end{aligned} \quad (3)$$

where $\mu_p = 2.79$ is the proton magnetic moment and $r_p = 0.84$ fm is the proton charge radius [16].

The density matrix of the photon emitted by the quark is

$$\begin{aligned} \rho_{\alpha\beta}^{(2)} &= -\frac{1}{2q_2^2} \text{Tr}\{\hat{p}'_2 \gamma_\alpha \hat{p}_2 \gamma_\beta\} \\ &= -\left(g_{\alpha\beta} - \frac{q_{2\alpha} q_{2\beta}}{q_2^2}\right) - \frac{(2p_2 - q_2)_\alpha (2p_2 - q_2)_\beta}{q_2^2}. \end{aligned} \quad (4)$$

It is convenient to consider the lepton pair production in the basis of virtual photon helicity states. In the center of mass system (c.m.s.) of the colliding photons, let $q_1 = (\tilde{\omega}_1, 0, 0, \tilde{q})$, $q_2 = (\tilde{\omega}_2, 0, 0, -\tilde{q})$. The standard set of orthonormal four-vectors orthogonal to q_1 and q_2 is

$$\begin{aligned} e_1^+ &= \frac{1}{\sqrt{2}}(0, -1, -i, 0), & e_1^- &= \frac{1}{\sqrt{2}}(0, 1, -i, 0), & e_1^0 &= \frac{i}{\sqrt{-q_1^2}}(\tilde{q}, 0, 0, \tilde{\omega}_1), \\ e_2^+ &= \frac{1}{\sqrt{2}}(0, 1, -i, 0), & e_2^- &= \frac{1}{\sqrt{2}}(0, -1, -i, 0), & e_2^0 &= \frac{i}{\sqrt{-q_2^2}}(-\tilde{q}, 0, 0, \tilde{\omega}_2). \end{aligned} \quad (5)$$

Due to the conservation of vector current, the covariant density matrices $\rho_i^{\mu\nu}$ satisfy $q_1^\mu \rho_1^{\mu\nu} = q_2^\mu \rho_2^{\mu\nu} = 0$. Thus, we can write

$$\rho_i^{\mu\nu} = \sum_{a,b} (e_i^{a\mu})^* e_i^{b\nu} \rho_i^{ab}, \quad (6)$$

$$\rho_i^{ab} = (-1)^{a+b} e_i^{a\mu} (e_i^{b\nu})^* \rho_i^{\mu\nu}, \quad (7)$$

where $a, b \in \{\pm 1, 0\}$, and ρ_i^{ab} are the density matrices in the helicity representation. The amplitudes of the lepton pair production in the helicity basis M_{ab} appear from the following equation:

$$\begin{aligned} & \rho_1^{\mu\nu} \rho_2^{\alpha\beta} M_{\mu\alpha} M_{\nu\beta}^* \\ &= (-1)^{a+b+c+d} \rho_1^{ab} \rho_2^{cd} M_{ac} M_{bd}^* \\ &= \rho_{++}^{(1)} \rho_{++}^{(2)} |M_{++}|^2 + \rho_{++}^{(1)} \rho_{--}^{(2)} |M_{+-}|^2 + \rho_{++}^{(1)} \rho_{00}^{(2)} |M_{+0}|^2 \\ & \quad + \rho_{--}^{(1)} \rho_{++}^{(2)} |M_{-+}|^2 + \rho_{--}^{(1)} \rho_{00}^{(2)} |M_{-0}|^2 + \rho_{--}^{(1)} \rho_{--}^{(2)} |M_{--}|^2. \end{aligned} \quad (8)$$

In this expression nondiagonal terms (those with $a \neq b$ or $c \neq d$) originated from the interference are omitted since their contributions cancel out when one integrates over azimuthal angles of the proton and the quark in the final state [15,17]. The contribution of the longitudinally polarized photon emitted by the proton is neglected since it is proportional to Q_1^2/W^2 , where W is the invariant mass of the produced lepton pair. The reason is that due to the elastic form factors Q_1^2 is bounded by approximately $(200 \text{ MeV})^2$ [7] while Z boson exchange corrections become noticeable at $Q_1^2 \sim M_Z^2$.

Matrix elements of the photon density matrices in the helicity representation for transverse polarizations were found in [10] (see also [15,17]). For the first photon we have

$$\rho_{++}^{(1)} = \rho_{--}^{(1)} \approx D(Q_1^2) \frac{2E^2 q_{1\perp}^2}{\omega_1^2 Q_1^2}, \quad (9)$$

where E is the proton energy in the c.m.s. of the colliding protons, $q_{1\perp}$ is the transversal momentum of the photon, and ω_1 is its energy in the same system. The function $D(Q_1^2)$ is defined in (2). In the following we will calculate the cross section of the muon pair production in the parton model. For the second photon, which is emitted by the quark with the initial energy xE , $0 < x < 1$, we have

$$\rho_{++}^{(2)} = \rho_{--}^{(2)} = \frac{2x^2 E^2 q_{2\perp}^2}{\omega_2^2 Q_2^2}, \quad \rho_{00}^{(2)} = \frac{4x^2 E^2 q_{2\perp}^2}{\omega_2^2 Q_2^2}. \quad (10)$$

Changing the integration variables from $d^3 p'_1 d^3 p'_2$ to $d^3 q_1 d^3 q_2 = 2\pi(1/2) dq_{1\perp}^2 d\omega_1 \cdot 2\pi(1/2) dq_{2\perp}^2 d\omega_2$ and substituting expressions (8)–(10) in (1), we get

$$\begin{aligned} d\sigma_{pq \rightarrow p\mu^+\mu^-q} &= 2Q_q^2 (4\pi\alpha)^2 \frac{q_1 q_2}{p_1 p_2} D(Q_1^2) \frac{2E^2 2x^2 E^2}{\omega_1^2 \omega_2^2} \sigma_{\gamma\gamma^* \rightarrow \mu^+\mu^-} \cdot \frac{q_{1\perp}^2 \frac{1}{2} dq_{1\perp}^2 d\omega_1}{Q_1^4 (2\pi)^2 2E} \cdot \frac{q_{2\perp}^2 \frac{1}{2} dq_{2\perp}^2 d\omega_2}{Q_2^4 (2\pi)^2 2Ex} f_q(x, Q_2^2) dx \\ &= 2 \cdot \left(\frac{\alpha}{\pi}\right)^2 Q_q^2 \frac{q_1 q_2}{p_1 p_2} \sigma_{\gamma\gamma^* \rightarrow \mu^+\mu^-} x E^2 \frac{D(Q_1^2) q_{1\perp}^2 dq_{1\perp}^2}{Q_1^4} \frac{q_{2\perp}^2 dq_{2\perp}^2}{Q_2^4} \frac{d\omega_1 d\omega_2}{\omega_1^2 \omega_2^2} f_q(x, Q_2^2) dx, \end{aligned} \quad (11)$$

where $\sigma_{\gamma\gamma^* \rightarrow \mu^+\mu^-}$ is the cross section of $\mu^+\mu^-$ production in $\gamma\gamma^*$ collision, $q_1 q_2 = (W^2 - q_2^2)/2$ and $p_1 p_2 = 2E^2 x$. The differential cross section of muon pair production in the c.m.s. of the photons is

$$\begin{aligned} d\sigma_{\gamma\gamma^* \rightarrow \mu^+\mu^-} &= \frac{\sum |\overline{M}|^2 d\cos\theta}{32\pi W^2 (1 + Q_2^2/W^2)}, \\ \sum |\overline{M}|^2 &= \frac{1}{4} [|M_{++}|^2 + |M_{+-}|^2 + |M_{-+}|^2 + |M_{--}|^2 + 2|M_{+0}|^2 + 2|M_{-0}|^2], \end{aligned} \quad (12)$$

where M_{ab} are the amplitudes of the process $\gamma\gamma^* \rightarrow \mu^+\mu^-$ in the helicity representation, θ is the scattering angle. It is convenient to express the corresponding cross section as the sum of the terms with the photon emitted by the quark polarized transversely and longitudinally: $\sigma_{\gamma\gamma^* \rightarrow \mu^+\mu^-} = \sigma_{TT} + \sigma_{TS}$, where according to Eq. (E3) from [15]

$$\begin{aligned} \sigma_{TS} &\equiv \int \frac{1}{2} [|M_{+0}|^2 + |M_{-0}|^2] \frac{d\cos\theta}{32\pi W^2 (1 + Q_2^2/W^2)} \approx \frac{16\pi\alpha^2 W^2 Q_2^2}{(W^2 + Q_2^2)^3}, \\ \sigma_{TT} &\equiv \int \frac{1}{4} [|M_{++}|^2 + |M_{+-}|^2 + |M_{-+}|^2 + |M_{--}|^2] \frac{d\cos\theta}{32\pi W^2 (1 + Q_2^2/W^2)} \\ &\approx \frac{4\pi\alpha^2}{W^2} \left[\frac{1 + Q_2^4/W^4}{(1 + Q_2^2/W^2)^3} \ln \frac{W^2}{m^2} - \frac{(1 - Q_2^2/W^2)^2}{(1 + Q_2^2/W^2)^3} \right], \end{aligned} \quad (13)$$

where m is the muon mass.¹ Integration of (11) with respect to $q_{1\perp}^2$ factors out the equivalent photon spectrum of the proton [[10], Eqs. (4) and (5)]

$$n_p(\omega_1) = \frac{\alpha}{\pi\omega_1} \int_0^\infty \frac{D(Q_1^2)q_{1\perp}^2 dq_{1\perp}^2}{Q_1^4} \\ = \frac{\alpha}{\pi\omega_1} \left\{ \left(1 + 4u - (\mu_p^2 - 1) \frac{u}{v} \right) \ln \left(1 + \frac{1}{u} \right) - \frac{24u^2 + 42u + 17}{6(u+1)^2} \right. \\ \left. - \frac{\mu_p^2 - 1}{(v-1)^3} \left[\frac{1+u/v}{v-1} \ln \frac{u+v}{u+1} - \frac{6u^2(v^2 - 3v + 3) + 3u(3v^2 - 9v + 10) + 2v^2 - 7v + 11}{6(u+1)^2} \right] \right\}, \quad (14)$$

where $u = (\omega_1/\Lambda\gamma)^2$, $v = (2m_p/\Lambda)^2$, $q_1^2 \equiv -Q_1^2 \approx -q_{1\perp}^2 - \omega_1^2/\gamma^2$, and $\gamma = E/m_p$.

It is convenient to change the integration variables in (11) from the photon energies ω_1 and ω_2 to the square of the invariant mass of the produced pair $W^2 = 4\omega_1\omega_2 + q_2^2$ and its rapidity $y = (1/2) \ln \omega_1/\omega_2$: $d\omega_1 d\omega_2 dq_{2\perp}^2 = (1/4) dW^2 dy dQ_2^2$. Taking into account that $q_2^2 \equiv -Q_2^2 \approx -q_{2\perp}^2 - \omega_2^2/\gamma^2$, where $\gamma_q = E_q/m_q \approx 3xE/m_p = 3x\gamma$,² we obtain

$$d\sigma_{pq \rightarrow p\mu^+\mu^-q} = \frac{\alpha}{2\pi} Q_q^2 n_p(\omega_1) \sigma_{\gamma\gamma^* \rightarrow \mu^+\mu^-}(W^2, Q_2^2) \\ \times \frac{Q_2^2 - (\omega_2/3x\gamma)^2}{\omega_2 Q_2^4} dW^2 dy dQ_2^2 f_q(x, Q_2^2) dx, \quad (15)$$

where $\omega_1 = \sqrt{W^2 + Q_2^2} \cdot e^y/2$, $\omega_2 = \sqrt{W^2 + Q_2^2} \cdot e^{-y}/2$.

When we were considering this process in [10], we were working under experimental constraints that allowed us to use the approximation $Q_2^2 \ll W^2$. In that case the photon emitted by the quark is approximately real, the cross section for the photon fusion does not depend on Q_2^2 , and we could factor out the function that we loosely interpreted as the equivalent photon spectrum of quark q :

$$n_q(\omega) = \frac{2\alpha Q_q^2}{\pi\omega} \int_{\omega/E}^1 dx \int_0^{p_T^{\mu\mu}} dq_{2\perp} \frac{q_{2\perp}^3}{Q_2^4} f_q(x, Q_2^2), \quad (16)$$

where $p_T^{\mu\mu} = 5$ GeV is the experimental constraint on the muon system transversal momentum imposed in [10]. We can use an analogous function here to simplify Eq. (15) and to make it obvious how the violation of the equivalent photon approximation occurs in this problem:

¹Calculation of electroweak loop corrections to the $\gamma\gamma \rightarrow \ell^+\ell^-$ cross section can be found in the literature, see for example [18].

²Since the quark is bound within proton, we use the constituent quark mass $m_q = m_p/3 \approx 300$ MeV [[19] (60.1)]. In [10] it was checked that variation of m_q from 200 to 400 MeV changes the value of the cross section by few percents.

$$n_q(\omega_2) = \frac{\alpha Q_q^2}{\pi\omega_2} \int dx \int dQ_2^2 \frac{q_{2\perp}^2}{Q_2^4} f_q(x, Q_2^2), \quad (17)$$

$$\frac{dn_q(\omega_2)}{dQ_2^2} = \frac{\alpha Q_q^2}{\pi\omega_2} \int_{x_{\min}}^1 \frac{Q_2^2 - (\omega_2/3x\gamma)^2}{Q_2^4} f_q(x, Q_2^2) dx, \quad (18)$$

where

$$x_{\min} = \sqrt{\frac{W^2 + Q_2^2}{s}} \cdot e^{-y} \cdot \max \left\{ 1, \frac{m_p}{3\sqrt{Q_2^2}} \right\}, \quad (19)$$

$s = 4E^2$ is the Mandelstam variable of the $pp \rightarrow p\mu^+\mu^-X$ reaction. In this way from (15) we obtain:

$$\sigma_{pq \rightarrow p\mu^+\mu^-q} = \frac{1}{2} \int_{\hat{W}^2}^s dW^2 \int_{\frac{W^4}{36\gamma^2 s}}^{s-W^2} \sigma_{\gamma\gamma^* \rightarrow \mu^+\mu^-}(W^2, Q_2^2) dQ_2^2 \\ \times \int_{\frac{1}{2} \ln \left(\frac{s}{W^2 + Q_2^2} \right)}^{\frac{1}{2} \ln \frac{s}{W^2 + Q_2^2}} \left(\frac{W^2 + Q_2^2}{s} \right)^{\max \left(1, \frac{m_p^2}{9Q_2^2} \right)} n_p(\omega_1) \frac{dn_q(\omega_2)}{dQ_2^2} dy, \quad (20)$$

where we assume the experimental constraint on the invariant mass of the muon pair $W > \hat{W} = 10$ GeV.

Finally, summing over valent u and d and sea quarks we get:

$$\sigma_{pp \rightarrow p\mu^+\mu^-X} = \sum_q \sigma_{pq \rightarrow p\mu^+\mu^-q}. \quad (21)$$

III. Z BOSON EXCHANGE CORRECTIONS

Corrections to the described by Fig. 1 and (1) $\gamma\gamma$ -fusion reaction come from the interference with the two diagrams shown in Fig. 2 and from the square of these diagrams. In both cases the expression for the density matrix $\rho_{\alpha\beta}^{(2)}$ given by (4) should be modified in order to take into account the axial coupling of Z boson to quarks. Let us designate these matrices $\tilde{\rho}^{(2)}$ and $\tilde{\tilde{\rho}}^{(2)}$ correspondingly. Masses of quarks can be safely neglected making matrices $\tilde{\rho}^{(2)}$ and $\tilde{\tilde{\rho}}^{(2)}$

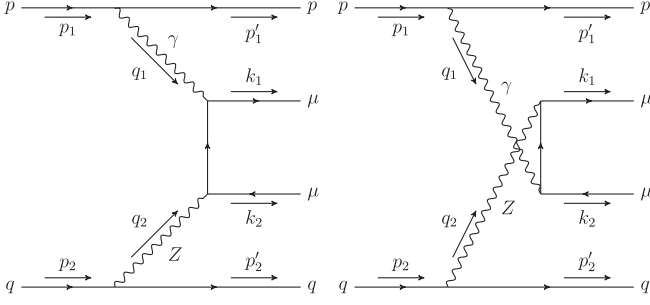


FIG. 2. Weak interaction corrections to muon pair production in semi-inclusive $pp \rightarrow p\mu^+\mu^-X$ reaction originating from the diagrams with Z boson exchange.

transversal: $\tilde{\rho}_{\alpha\beta}^{(2)} q_{2\beta} = \tilde{\rho}_{\alpha\beta}^{(2)} q_{2\beta} = 0$. That is why they can be expanded over the same 4-vectors $e_{2\mu}^a$, presented in (5). The coupling of Z boson to quarks equals

$$\Delta L_{qqZ} = \frac{e}{s_W c_W} \left[\frac{g_V^q}{2} \bar{q} \gamma_\alpha q + \frac{g_A^q}{2} \bar{q} \gamma_\alpha \gamma_5 q \right] Z_\alpha,$$

$$s_W \equiv \sin \theta_W, \quad c_W \equiv \cos \theta_W,$$

$$g_V^q = T_3^q - 2Q_q s_W^2, \quad g_A^q = T_3^q, \quad (22)$$

where $e = \sqrt{4\pi\alpha}$, θ_W is the electroweak mixing angle, $s_W^2 \approx 0.231$ [19], and T_3^q is the weak isospin of quark q , so for $\tilde{\rho}_{\alpha\beta}^{(2)}$ and $\tilde{\rho}_{\alpha\beta}^{(2)}$ we obtain

$$\tilde{\rho}_{\alpha\beta}^{(2)} = -\frac{1}{2q_2^2} \left[\frac{g_V^q}{2} \text{Tr} \{ \hat{p}'_2 \gamma_\alpha \hat{p}_2 \gamma_\beta \} + \frac{g_A^q}{2} \text{Tr} \{ \hat{p}'_2 \gamma_\alpha \hat{p}_2 \gamma_\beta \gamma_5 \} \right], \quad (23)$$

$$\tilde{\rho}_{\alpha\beta}^{(2)} = -\frac{1}{2q_2^2} \text{Tr} \left\{ \hat{p}'_2 \left(\frac{g_V^q}{2} \gamma_\alpha + \frac{g_A^q}{2} \gamma_\alpha \gamma_5 \right) \right. \\ \left. \times \hat{p}_2 \left(\frac{g_V^q}{2} \gamma_\beta + \frac{g_A^q}{2} \gamma_\beta \gamma_5 \right) \right\}. \quad (24)$$

Calculating matrix elements of $\tilde{\rho}_{ab}^{(2)}$ in the helicity representation according to (7), we get that the correction proportional to g_A^q cancels in $\tilde{\rho}_{00}^{(2)}$ and is proportional to xE/ω_2 in $\tilde{\rho}_{++}^{(2)}$ and $\tilde{\rho}_{--}^{(2)}$, so it can be neglected when compared to the contribution of the correction proportional to g_V^q which behaves as $(xE/\omega_2)^2$ [see (10)]. Therefore

$$\tilde{\rho}_{ab}^{(2)} \approx \frac{g_V^q}{2} \rho_{ab}^{(2)}. \quad (25)$$

In the case of $\tilde{\rho}_{\alpha\beta}^{(2)}$ we observe similar suppression of terms originating from the terms proportional to the product $g_A^q \cdot g_V^q$. Neglecting them we obtain

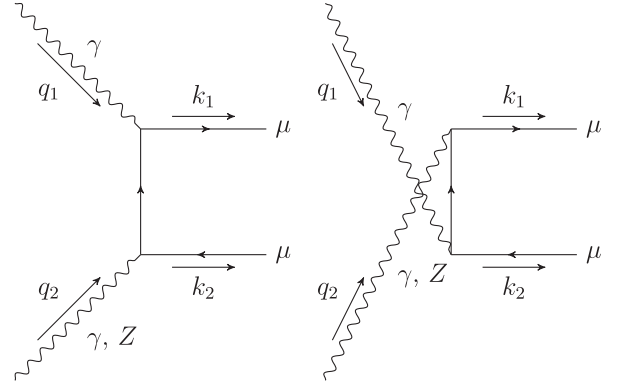


FIG. 3. $\mu^+\mu^-$ pair production in $\gamma\gamma$ (or γZ) fusion.

$$\tilde{\rho}_{ab}^{(2)} \approx \frac{(g_V^q)^2 + (g_A^q)^2}{4} \rho_{ab}^{(2)}. \quad (26)$$

The amplitude that corresponds to the sum of the diagrams in Figs. 1 and 2 equals

$$A = A_\mu \bar{p}' \gamma_\mu p / q_1^2,$$

$$A_\mu = \frac{e Q_q}{q_2^2} \bar{q}' \gamma_\alpha q M_{\mu\alpha}^\gamma + \frac{e}{s_W c_W (q_2^2 - M_Z^2)} \bar{q}' \\ \times \left[\frac{g_V^q}{2} \gamma_\alpha + \frac{g_A^q}{2} \gamma_\alpha \gamma_5 \right] q M_{\mu\alpha}^Z. \quad (27)$$

For the $\gamma\gamma \rightarrow \mu^+\mu^-$ and $\gamma Z \rightarrow \mu^+\mu^-$ amplitudes (see Fig. 3) we have

$$M_{\mu\alpha}^\gamma = Q_\mu^2 e^2 \left[\bar{\mu} \gamma_\mu \frac{1}{\hat{k}_1 - \hat{q}_1 - m} \gamma_\alpha \mu + \bar{\mu} \gamma_\alpha \frac{1}{\hat{q}_1 - \hat{k}_2 - m} \gamma_\mu \mu \right], \quad (28)$$

$$M_{\mu\alpha}^Z = \frac{Q_\mu e^2}{s_W c_W} \left\{ \frac{g_V^\mu}{2} \left[\bar{\mu} \gamma_\mu \frac{1}{\hat{k}_1 - \hat{q}_1 - m} \gamma_\alpha \mu \right. \right. \\ \left. \left. + \bar{\mu} \gamma_\alpha \frac{1}{\hat{q}_1 - \hat{k}_2 - m} \gamma_\mu \mu \right] + \frac{g_A^\mu}{2} [\gamma_\alpha \rightarrow \gamma_\alpha \gamma_5] \right\} \\ = \frac{1}{s_W c_W} \frac{g_V^\mu}{2 Q_\mu} M_{\mu\alpha}^\gamma + \frac{Q_\mu e^2}{s_W c_W} \frac{g_A^\mu}{2} \left[\bar{\mu} \gamma_\mu \frac{1}{\hat{k}_1 - \hat{q}_1 - m} \gamma_\alpha \gamma_5 \mu \right. \\ \left. + \bar{\mu} \gamma_\alpha \gamma_5 \frac{1}{\hat{q}_1 - \hat{k}_2 - m} \gamma_\mu \mu \right]. \quad (29)$$

Substituting (28) and (29) into (27) and separating the term proportional to $M_{\mu\alpha}^\gamma$, we obtain

$$\begin{aligned}
A_\mu = & \left\{ \bar{q}' \gamma_\alpha q \left(\frac{e Q_q Q_\mu^2}{q_2^2} + \frac{g_V^\mu}{2} \frac{e Q_\mu}{(s_W c_W)^2 (q_2^2 - M_Z^2)} \frac{g_V^q}{2} \right) + \bar{q}' \gamma_\alpha \gamma_5 q \frac{g_V^\mu}{2} \frac{e Q_\mu}{(s_W c_W)^2 (q_2^2 - M_Z^2)} \frac{g_A^q}{2} \right\} \\
& \times e^2 \left[\bar{\mu} \gamma_\mu \frac{1}{\hat{k}_1 - \hat{q}_1 - m} \gamma_\alpha \mu + \bar{\mu} \gamma_\alpha \frac{1}{\hat{q}_1 - \hat{k}_2 - m} \gamma_\mu \mu \right] + \bar{q}' \left(\frac{g_V^q}{2} \gamma_\alpha + \frac{g_A^q}{2} \gamma_\alpha \gamma_5 \right) q \frac{g_A^\mu}{2} \frac{e Q_\mu}{(s_W c_W) (q_2^2 - M_Z^2)} \frac{e^2}{s_W c_W} \\
& \times \left[\bar{\mu} \gamma_\mu \frac{1}{\hat{k}_1 - \hat{q}_1 - m} \gamma_\alpha \gamma_5 \mu + \bar{\mu} \gamma_\alpha \gamma_5 \frac{1}{\hat{q}_1 - \hat{k}_2 - m} \gamma_\mu \mu \right]. \tag{30}
\end{aligned}$$

The following two statements are proved in the Appendix: (1) the amplitudes in the square brackets which describe the vector and axial couplings to muons do not interfere and (2) the square of the amplitude with the axial coupling equals that with the vector coupling (we are working in $W \gg m$ domain). In this way for the square of the amplitude we get

$$\begin{aligned}
|\mathcal{A}|^2 & \equiv \kappa |\mathcal{A}_{\gamma\gamma}|^2, \\
\kappa(Q_2^2) & = 1 + 2 \cdot \frac{g_V^\mu}{Q_\mu} \cdot \frac{g_V^q}{Q_q} \cdot \lambda + \frac{(g_V^\mu)^2 + (g_A^\mu)^2}{Q_\mu^2} \\
& \cdot \frac{(g_V^q)^2 + (g_A^q)^2}{Q_q^2} \cdot \lambda^2, \tag{31}
\end{aligned}$$

$$\lambda \equiv \frac{1}{(2s_W c_W)^2 (1 + M_Z^2/Q_2^2)}, \tag{32}$$

where $\mathcal{A}_{\gamma\gamma}$ is the amplitude for the reaction via photon fusion only.

Thus we get that the squares of the helicity amplitudes describing the $\gamma\gamma^* \rightarrow \mu^+\mu^-$ reaction presented in (12) should be multiplied by the same factor κ in order to take into account the diagrams with the Z boson exchange. It is convenient to calculate the helicity amplitudes M^γ in the muons c.m.s.

The sum of the squares of the amplitudes of the processes with the longitudinal polarization of the vector boson (Z or photon) emitted by the quark is

$$|\tilde{M}_{+0}|^2 + |\tilde{M}_{-0}|^2 = (4\pi\alpha)^2 \frac{32Q_2^2}{W^2(1 + Q_2^2/W^2)^2} \kappa, \tag{33}$$

and the corresponding cross section is

$$\tilde{\sigma}_{TS} = \frac{16\pi\alpha^2 Q_2^2}{W^4(1 + Q_2^2/W^2)^3} \kappa. \tag{34}$$

It equals zero for $Q_2^2 = 0$, as it should be. For the contribution of the transversal amplitudes with opposite helicities we obtain

$$\begin{aligned}
|\tilde{M}_{+-}|^2 + |\tilde{M}_{-+}|^2 & = (4\pi\alpha)^2 \frac{4\sin^2\theta(1 + \cos^2\theta)}{(1 + Q_2^2/W^2)^2} \\
& \times \left[\frac{1}{1 - v \cos\theta} + \frac{1}{1 + v \cos\theta} \right]^2 \kappa. \tag{35}
\end{aligned}$$

Since the sum of helicities of the produced leptons equals 1, while that of the annihilating vector bosons equals 2, the production at $\theta = 0, \pi$ is forbidden by the helicity conservation. The factor $\sin\theta$ takes care of it. For the contribution to the cross section we obtain

$$\tilde{\sigma}_{+-} + \tilde{\sigma}_{-+} = \frac{4\pi\alpha^2}{W^2(1 + Q_2^2/W^2)^3} \left[\ln\left(\frac{W^2}{m^2}\right) - 2 \right] \kappa, \tag{36}$$

where m is a lepton mass.

Performing straightforward calculations, for the square of the amplitude induced by photons with helicities $e_{1,2}^\pm$ we obtain

$$\begin{aligned}
|M_{++}^\gamma|^2 & = 4(4\pi\alpha)^2 \left\{ \sin^2\theta \frac{Q_2^4/W^4}{(1 + Q_2^2/W^2)^2} \right. \\
& \times \left[\frac{1}{(1 - v \cos\theta)^2} + \frac{1}{(1 + v \cos\theta)^2} \right] \\
& \left. + \frac{1 - v^2}{(1 - v \cos\theta)^2} + \frac{1 - v^2}{(1 + v \cos\theta)^2} \right\}, \tag{37}
\end{aligned}$$

where v is the muon velocity in the c.m.s., $v^2 = 1 - 4m^2/W^2$. Helicity of the initial state of the two photons equals zero while for massless muons helicity of the $\mu^+\mu^-$ pair equals ± 1 . That is why the amplitude M_{++} should be zero at $\theta = 0, \pi$ when the helicity is conserved (massless muons). The factor $\sin^2\theta$ multiplying the first term in the curly braces takes care of this. In the case of muon (or antimuon) spin flip the final state will have zero helicity, and muons production at $\theta = 0, \pi$ is allowed. The two last terms in the curly braces are responsible for the forward and backward muon production. Though their numerators are proportional to m^2 , they make finite contribution to the cross section in the limit $m \rightarrow 0$ due to the denominators which come from muon propagators. Integrating these terms over θ , we obtain a finite in the limit $m/W \rightarrow 0$ contribution to the cross section which comes

from the $\theta \sim m/W$ and $\theta \sim \pi - m/W$ domains. This phenomenon is the essence of the chiral anomaly [20,21]: even in the limit $m \rightarrow 0$ production of muons at $\theta = 0, \pi$ is still allowed.

The contribution to the cross section of muon pair production is the following:

$$\begin{aligned} \tilde{\sigma}_{++} + \tilde{\sigma}_{--} &= \int \frac{1}{4} (|\tilde{M}_{++}|^2 + |\tilde{M}_{--}|^2) d\cos\theta \\ &= \frac{4\pi\alpha^2}{W^2(1 + Q_2^2/W^2)} \left[\frac{Q_2^4/W^4}{(1 + Q_2^2/W^2)^2} \right. \\ &\quad \left. \times \left(\ln \frac{W^2}{m^2} - 2 \right) + 1 \right] \chi \end{aligned} \quad (38)$$

and $\tilde{\sigma}_{TT} = \tilde{\sigma}_{+-} + \tilde{\sigma}_{-+} + \tilde{\sigma}_{++} + \tilde{\sigma}_{--}$, where $\tilde{\sigma}_{+-} + \tilde{\sigma}_{-+}$ is given by (36). Let us note that even in the case of the collision of real photons ($Q_2^2 = 0$) the cross section $\tilde{\sigma}_{++} + \tilde{\sigma}_{--}$ is nonzero. As a final result we get

$$\tilde{\sigma}_{TT} = \frac{4\pi\alpha^2}{W^2} \left[\frac{1 + Q_2^4/W^4}{(1 + Q_2^2/W^2)^3} \ln \frac{W^2}{m^2} - \frac{(1 - Q_2^2/W^2)^2}{(1 + Q_2^2/W^2)^3} \right] \chi. \quad (39)$$

We have discussed $\gamma\gamma$ and γZ contributions. Let us note that the ZZ contribution should be very small for the

process under consideration since it is suppressed by $Q_1^2/M_Z^2 \lesssim 10^{-5}$.

IV. NUMERICAL RESULTS

Replacing in (20) $\sigma_{\gamma\gamma^* \rightarrow \mu^+ \mu^-}(W^2, Q_2^2)$ with $\tilde{\sigma}_{TS} + \tilde{\sigma}_{TT}$ given in (33) and (39) we obtain an expression for the differential cross section of a muon pair production which takes into account the Z boson exchange:

$$\begin{aligned} \frac{d\sigma_{pp \rightarrow p\mu^+ \mu^- X}}{dW} &= \frac{4\alpha W}{\pi} \sum_q Q_q^2 \int_{\frac{W^4}{36\gamma^2 s}}^{s-W^2} \frac{[\tilde{\sigma}_{TS}(W^2, Q_2^2) + \tilde{\sigma}_{TT}(W^2, Q_2^2)]}{W^2 + Q_2^2} dQ_2^2 \\ &\quad \times \int_{\frac{1}{2} \ln \frac{s}{W^2 + Q_2^2}}^{\frac{1}{2} \ln \frac{s}{Q_2^2}} \omega_1 n_p(\omega_1) dy \\ &\quad \times \int_{x_{\min}}^1 \frac{Q_2^2 - (\omega_2/3x\gamma)^2}{Q_2^4} f_q(x, Q_2^2) dx, \end{aligned} \quad (40)$$

where we used the equality $\omega_2 = (W^2 + Q_2^2)/4\omega_1$.

For better convergence of the numerical integration it is convenient to change the order of integrals:

$$\begin{aligned} \frac{d\sigma_{pp \rightarrow p\mu^+ \mu^- X}}{dW} &= \frac{4\alpha W}{\pi} \sum_q Q_q^2 \int_{\frac{W^4}{36\gamma^2 s}}^{s-W^2} \frac{\sigma_{\gamma\gamma^* \rightarrow \mu^+ \mu^-}(W^2, Q_2^2)}{(W^2 + Q_2^2) Q_2^4} \cdot \chi(Q_2^2) \cdot dQ_2^2 \\ &\quad \times \int_{\frac{W^2 + Q_2^2}{s} \max\left(1, \frac{m_p}{3\sqrt{Q_2^2}}\right)}^1 dx f_q(x, Q_2^2) \int_{\frac{1}{2} \ln \frac{s}{W^2 + Q_2^2}}^{\frac{1}{2} \ln \frac{s}{Q_2^2}} \omega_1 n_p(\omega_1) [Q_2^2 - (\omega_2/3x\gamma)^2] dy, \end{aligned} \quad (41)$$

$$\begin{aligned} \chi(Q_2^2) &= 1 + 2 \cdot \frac{g_V^\mu}{Q_\mu} \cdot \frac{g_V^q}{Q_q} \cdot \lambda + \frac{(g_V^\mu)^2 + (g_A^\mu)^2}{Q_\mu^2} \\ &\quad \cdot \frac{(g_V^q)^2 + (g_A^q)^2}{Q_q^2} \cdot \lambda^2, \end{aligned} \quad (42)$$

$$\lambda \equiv \frac{1}{(2s_W c_W)^2 (1 + M_Z^2/Q_2^2)}. \quad (43)$$

In this formula we explicitly separated $\chi(Q_2^2)$ since it is the only source of weak interaction corrections in (41). For all charged fermions in the Standard Model g_V and g_A have the same sign as their charge Q , so the weak interaction correction is positive.

Let us make a couple of comments regarding formula (41) and its accuracy. The lower integration limit on Q_2^2 in (41) is much smaller than $(1 \text{ GeV})^2$. So we should explain if it is consistent with the parton approximation.

This lower limit comes from kinematics and does not take into account other requirements. However, there is a smooth cut at small Q_2^2 in the parton distribution functions provided by LHAPDF [22] so we decided not to change this limit in (41). We have checked how the results depend on Q_2^2 lower limit. Since $\sigma_{\gamma\gamma^* \rightarrow \mu^+ \mu^-}(W^2, Q_2^2)$ rapidly decreases for $Q_2^2 \gtrsim W^2$ (i.e., main contribution comes from $Q_2^2 \lesssim W^2$), the impact of low- Q_2^2 is more pronounced for smaller W . For $W = 20 \text{ GeV}$ we checked that region $Q_2^2 > (1 \text{ GeV})^2$ gives 85% of the integral, $Q_2^2 > (0.5 \text{ GeV})^2$ gives 96.6%, while $Q_2^2 > (0.25 \text{ GeV})^2$ gives 99.4% which is already close to the required relative numerical precision (10^{-3}). Results for $Q_2^2 > (0.01 \text{ GeV})^2$ are well inside the required accuracy and give the value of the integral. All values in the paper correspond to the full integral calculation (without the extra cut on Q_2^2) while this ambiguity in where we should make the cut on Q_2^2 is treated as the uncertainty. We must stress that it does not affect the

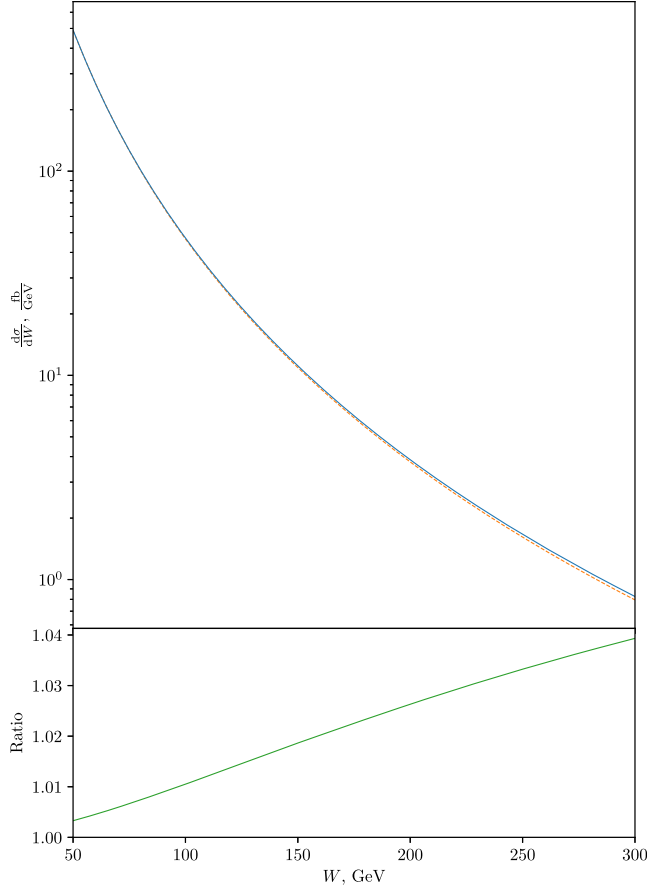


FIG. 4. Upper plot: differential cross section of the photon fusion only (orange dashed line) and with the weak interaction correction added (blue solid line). Lower plot: their ratio.

absolute value of the weak interaction correction since $\kappa(Q_2^2) = 1$ for $Q_2^2 \lesssim (1 \text{ GeV})^2$ with very good accuracy.

Another important source of uncertainty is parton distribution functions. We checked different PDFs: `cteq66` [23], `MMHT2014nnlo68cl` [24], `PDF4LHC15_nnlo_100` [25], `MSHT20nnlo_as118` [26]. The maximum variation for $W = 20 \text{ GeV}$ is about 6% which is rather significant. We use `MMHT2014nnlo68cl` for the calculations in this paper.

We should also note that the photon flux of the disintegrating proton is not fully described by the parton approximation. Resonance phenomena and other effects can increase the cross section by 10–15% [27–29]. However, the corresponding region $Q_2^2 \sim (1 \text{ GeV})^2$ is not relevant for the weak interaction correction, so we do not take these effects into account.

Results of our numerical calculation are shown in Fig. 4. We see that the weak interaction correction does not give a noticeable increase in the cross section. The reason for that is clear: all scales of Q_2^2 in (41) are equally important while for the weak interaction correction only the domain $M_Z^2 \lesssim Q_2^2 \lesssim W^2$ is relevant.

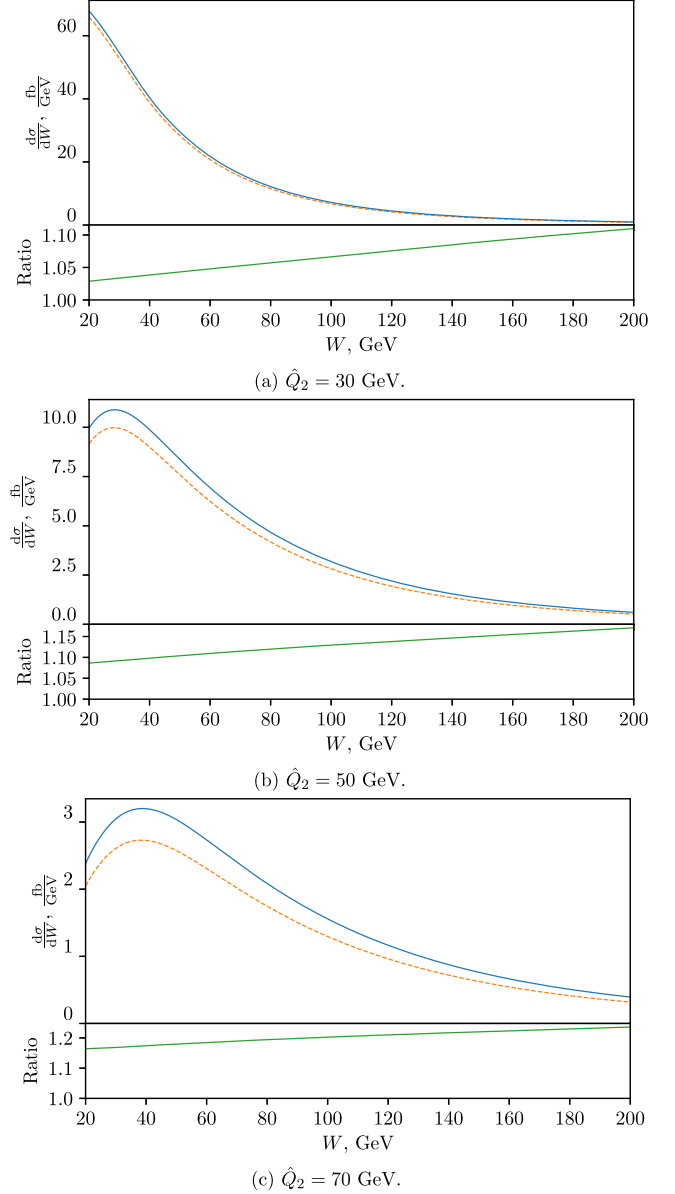


FIG. 5. Differential cross sections for different lower limits on Q_2^2 . Styles and colors of the lines are the same as in Fig. 4.

The weak interaction correction is more pronounced when we set the lower limit on Q_2^2 , $Q_2^2 > \hat{Q}_2^2$, closer to the electroweak scale, M_Z^2 . For $\hat{Q}_2 \gg 1 \text{ GeV}$ it means a cut on the total transverse momentum of the produced pair, $p_T^{\mu\mu} > \hat{Q}_2$. Such a selection is both theoretically and experimentally clean. From the theory side we have no complications due to low- Q^2 physics. From the experiment side this selection means high- p_T events with two distinguishable muons [at least for $W \gtrsim \hat{Q}_2$ since the cross section is additionally suppressed for $Q_2^2 > W^2$, see (41)]. The results for $\hat{Q}_2 = 30, 50, 70 \text{ GeV}$ are shown in Fig. 5. We see that the weak interaction correction reaches 20%.

When the lower limit on the total transverse momentum of the produced pair is set closer to the electroweak scale, most of the discussed uncertainties due to the low- Q^2 physics vanish, so we should discuss the accuracy of our result.

For $Q_2^2 \gtrsim M_Z^2$ the value of $\kappa(Q_2^2)$ very weakly depends on Q_2^2 and is mostly defined by electroweak mixing parameters. Thus, the value of the relative correction is more or less fixed, at least at the tree level. However, there are sources of uncertainties that should be discussed.

Since $\kappa(Q_2^2)$ is different for up- and down-type quarks, there is uncertainty due to the PDFs. Variation of PDF sets affects both absolute values and relative correction, however its effect is not as pronounced as it was at low Q_2^2 . For $\hat{Q}_2 = 70$ GeV and $W = 200$ GeV, variation over the same sets gives 1.6% uncertainty in the absolute values and 1.2% in the relative correction.

Higher orders of perturbation theory may lead to effective shift in Q^2 so structure functions should be taken at different Q_2^2 . Thus we should study how sensitive our results are to such kind of shifts. In order to do that we substituted $f_q(x, Q_2^2)$ by $f_q(x, 2Q_2^2)$ and $f_q(x, Q_2^2/2)$ in (41), and for $\hat{Q}_2 = 70$ GeV and $W = 20$ GeV got 2.4% increase and decrease in absolute values correspondingly.

In the limit $Q_2^2 \gg M_Z^2$ the function $\kappa(Q_2^2)$ reaches its maximum value:

$$\begin{aligned} \kappa(Q_2^2) &\approx 1 + 2 \cdot \frac{g_V^\mu}{Q_\mu} \cdot \frac{g_V^q}{Q_q} \cdot \frac{1}{(2s_W c_W)^2} + \frac{(g_V^\mu)^2 + (g_A^\mu)^2}{Q_\mu^2} \\ &\cdot \frac{(g_V^q)^2 + (g_A^q)^2}{Q_q^2} \cdot \frac{1}{(2s_W c_W)^4} \\ &\approx \begin{cases} 1.35 & \text{for } q = u, \bar{u}, c, \bar{c} \\ 2.76 & \text{for } q = d, \bar{d}, s, \bar{s}, b, \bar{b} \end{cases} \end{aligned} \quad (44)$$

However, to get an idea of what the correction in principle might be, one should know how much up- and down-type quarks contribute to the cross section in photon-photon fusion. From (18) we immediately see that the contributions into $\gamma\gamma$ fusion are proportional to the square of the quark charge, so up-type quarks give four times more even for the same density. In the large- x limit only valent quarks remain, and there are twice more u quarks than d quarks so in the $\gamma\gamma$ fusion cross section they should contribute in 8:1 ratio. However, at small x sea quarks slightly change this situation. We calculated individual contributions of each quark into the cross section (41) with κ set to 1 to get $\gamma\gamma$ fusion only. For $\hat{Q}_2 = 70$ GeV and $W = 20$ GeV, u quark gives 41% of the cross section, \bar{u} gives 16%, d —7%, \bar{d} —4%, s + \bar{s} —7%, c + \bar{c} —21%, b + \bar{b} —4%. Up-type quarks combined ($u + \bar{u} + c + \bar{c}$) give 78%. At $W = 200$ GeV up-type quarks give 80% of the cross section, so the asymptotic value $8/9 \approx 89\%$ is approached very slowly. Consequently, the asymptotic value of the

enhancement is $0.78 \times 1.35 + 0.22 \times 2.76 \approx 1.6$ (for the 8:1 ratio we would get 1.5).

V. CONCLUSIONS

We have calculated the weak interaction correction to the cross section of lepton pair production in semiexclusive process. Beforehand it was not obvious if this correction is significant or not. It turned out that it gives few percent increase of the production cross section. However, if we set the lower limit on the net transverse momentum of the produced pair, the correction goes up and can reach 20%.

ACKNOWLEDGMENTS

Numerical calculations were performed with the help of LIBEPA [30]. We are supported by RSF Grant No. 19-12-00123-II.

APPENDIX

Let us prove that the square of the expression in the square brackets in (30) that contains the product of the vector currents $\gamma_\mu \cdot \gamma_\alpha$ equals that which contains the product of the vector and axial currents $\gamma_\mu \cdot \gamma_\alpha \gamma_5$. This statement is evident for massless muons, $m = 0$. Thus taking into account the nonzero mass it is convenient to commute the muons propagators with the vector current γ_μ :

$$\bar{\mu}_1 \gamma_\mu (\hat{k}_1 - \hat{q}_1 + m) = \bar{\mu}_1 (2k_{1\mu} - \gamma_\mu \hat{q}_1), \quad (A1)$$

$$(\hat{q}_1 - \hat{k}_2 + m) \gamma_\mu \bar{\mu}_2 = (\hat{q}_1 \gamma_\mu - 2k_{2\mu}) \bar{\mu}_2. \quad (A2)$$

Then the mass remains only in the muons polarization density matrices from which two types of terms can give nonzero contribution to the cross section: $\sim \hat{k}_1 \hat{k}_2$ and $\sim m^2$. The terms proportional to the product of the momenta are the same for the vector-vector currents product and the vector-axial currents product, while those proportional to m^2 have the opposite signs. Let us prove that contributions of the terms proportional to m^2 are negligible.

In order to produce finite contributions in the limit $m^2/W^2 \rightarrow 0$ they should contain squares of the muon propagators $\sim 1/(k_1 q_1)^2$ or $1/(k_2 q_1)^2$. The terms proportional to $m^2/(k_1 q_1)^2$ are multiplied by $\text{Tr}[(2k_{1\mu} - \gamma_\mu \hat{q}_1) \gamma_\alpha \gamma_\beta \times (2k_{1\nu} - \hat{q}_1 \gamma_\nu)]$. For the amplitudes $M_{\pm 0}$ we get

$$\text{Tr}[(2k_{1\mu} - \gamma_\mu \hat{q}_1) \hat{e}_2^0 \hat{e}_2^0 (2k_{1\nu} - \hat{q}_1 \gamma_\nu)] = 16k_{1\mu} k_{1\nu}, \quad (A3)$$

where we take into account that $q_{1\mu} M_{\mu\alpha} = q_{1\nu} M_{\nu\beta} = 0$ and neglect q_1^2 . Since $k_{1\mu} e_{1\mu}^\pm \sim \sin \theta$, even for the scattering angles $\theta \sim 0$ or π we obtain negligible contribution into differential cross section $\sim m^2/W^2 \cdot \sin^2 \theta / (1 \pm v \cos \theta)^2$. Analogous consideration is valid for the term proportional to $1/(k_2 q_1)^2$.

In the case of transversal polarization of the photon or the Z boson emitted by the quark, the trace discussed above contains a sum of terms proportional to q_1^2 , $(q_1 e_2^\pm) = 0$, $(q_1 e_1^\pm) = 0$, and $(k_{1\mu} e_{1\mu}^\pm)(k_{1\nu} e_{1\nu}^\pm) \sim \sin^2 \theta$. In this way we demonstrate that the terms proportional to m^2 can be safely neglected which proves that the square of the amplitude which contains axial coupling equals that which contains only vector couplings.

It remains to prove that the amplitudes in the square brackets in (30) do not interfere. Let us multiply the expressions in the square brackets by the vector boson polarization vectors (5) and introduce notations M_{ik}^V and M_{ik}^A for the terms in the first and the second square brackets correspondingly. Using the identity $\text{Tr}[\gamma_A \gamma_B \dots \gamma_C \gamma_D] = \text{Tr}[\gamma_D \gamma_C \dots \gamma_B \gamma_A]$ one can check that the following relations are valid:

$$M_{++}^V [M_{++}^A]^* + M_{--}^A [M_{--}^V]^* = M_{++}^A [M_{++}^V]^* + M_{--}^V [M_{--}^A]^* = 0, \quad (\text{A4})$$

$$M_{+0}^V [M_{+0}^A]^* + M_{-0}^A [M_{-0}^V]^* = M_{+0}^A [M_{+0}^V]^* + M_{-0}^V [M_{-0}^A]^* = 0, \quad (\text{A5})$$

$$M_{+-}^V [M_{+-}^A]^* + M_{-+}^A [M_{-+}^V]^* = M_{+-}^A [M_{+-}^V]^* + M_{-+}^V [M_{-+}^A]^* = 0. \quad (\text{A6})$$

These relations are the consequence of the different behavior of the vector and axial helicity amplitudes under the P -parity inversion: for example, $M_{+-}^V \xrightarrow{P} -M_{-+}^V$ and $M_{+-}^A \xrightarrow{P} M_{-+}^A$. It follows that in the cross section the interference terms cancel.

-
- [1] The ATLAS Collaboration, Measurement of the exclusive $\gamma\gamma \rightarrow \mu^+\mu^-$ process in proton-proton collisions at $\sqrt{s} = 13$ TeV with the ATLAS detector, *Phys. Lett. B* **777**, 303 (2018).
- [2] S. I. Godunov, V. A. Novikov, A. N. Rozanov, M. I. Vysotsky, and E. V. Zhemchugov, Production of heavy charged particles in proton-proton ultraperipheral collisions at the Large Hadron Collider: Survival factor, *J. High Energy Phys.* **10** (2021) 234.
- [3] M. Bähr, S. Gieseke, M. A. Gigg, D. Grellscheid *et al.*, Herwig++ physics and manual, *Eur. Phys. J. C* **58**, 639 (2008).
- [4] J. Bellm, S. Gieseke, D. Grellscheid, S. Plätzer *et al.*, Herwig 7.0/Herwig++ 3.0 release note, *Eur. Phys. J. C* **76**, 196 (2016).
- [5] M. Dyndal and L. Schoeffel, The role of finite-size effects on the spectrum of equivalent photons in proton-proton collisions at the LHC, *Phys. Lett. B* **741**, 66 (2015).
- [6] L. A. Harland-Lang, V. A. Khoze, and M. G. Ryskin, Exclusive physics at the LHC with SuperChic 2, *Eur. Phys. J. C* **76**, 9 (2016).
- [7] M. Vysotsky and E. Zhemchugov, Equivalent photons in proton-proton and ion-ion collisions at the Large Hadron Collider, *Phys. Usp.* **62**, 910 (2019).
- [8] The CMS and TOTEM Collaborations, Observation of proton-tagged, central (semi)exclusive production of high-mass lepton pairs in pp collisions at 13 TeV with the CMS-TOTEM precision proton spectrometer, *J. High Energy Phys.* **07** (2018) 153.
- [9] The ATLAS Collaboration, Observation and measurement of forward proton scattering in association with lepton pairs produced via the photon fusion mechanism at ATLAS, *Phys. Rev. Lett.* **125**, 261801 (2020).
- [10] S. I. Godunov, E. K. Karkaryan, V. A. Novikov, A. N. Rozanov, M. I. Vysotsky, and E. V. Zhemchugov, pp scattering at the LHC with the lepton pair production and one proton tagging, *Eur. Phys. J. C* **82**, 1055 (2022).
- [11] S. I. Godunov, E. K. Karkaryan, V. A. Novikov, A. N. Rozanov, M. I. Vysotsky, and E. V. Zhemchugov, Forward proton scattering in association with muon pair production via the photon fusion mechanism at the LHC, *JETP Lett.* **115**, 59 (2022).
- [12] The Muon $g - 2$ Collaboration, Measurement of the positive muon anomalous magnetic moment to 0.46 ppm, *Phys. Rev. Lett.* **126**, 141801 (2021).
- [13] The Muon $g - 2$ Collaboration, Final report of the E821 muon anomalous magnetic moment measurement at BNL, *Phys. Rev. D* **73**, 072003 (2006).
- [14] L. A. Harland-Lang, Physics with leptons and photons at the LHC, *Phys. Rev. D* **104**, 073002 (2021).
- [15] V. M. Budnev, I. F. Ginzburg, G. V. Meledin, and V. G. Serbo, The two-photon particle production mechanism. Physical problems. Applications. Equivalent photon approximation, *Phys. Rep.* **15**, 181 (1975).
- [16] E. Tiesinga, P. J. Mohr, D. B. Newell, and B. N. Taylor, CODATA recommended values of the fundamental physical constants: 2018, *Rev. Mod. Phys.* **93**, 025010 (2021).
- [17] A. Dobrovolskaya and V. Novikov, On heavy Higgs boson production, *Z. Phys. C* **52**, 427 (1991).
- [18] M. Demirci and M. F. Mustamin, One-loop electroweak radiative corrections to charged lepton pair production in photon-photon collisions, *Phys. Rev. D* **103**, 113004 (2021).
- [19] Particle Data Group, Review of particle physics, *Prog. Theor. Exp. Phys.* **2022**, 083C01 (2022).

- [20] S. Adler, Axial-vector vertex in spinor electrodynamics, *Phys. Rev.* **177**, 2426 (1969).
- [21] J. Bell and R. Jackiw, A PCAC puzzle: $\pi^0 \rightarrow \gamma\gamma$ in the σ -model, *Nuovo Cimento A* **60**, 47 (1969).
- [22] A. Buckley, J. Ferrando, S. Lloyd, K. Nordström, B. Page, M. Rüfenacht, M. Schönherr, and G. Watt, LHAPDF6: Parton density access in the LHC precision era, *Eur. Phys. J. C* **75**, 132 (2015).
- [23] P. M. Nadolsky, H. L. Lai, Q. H. Cao, J. Huston, J. Pumplin, D. Stump, W. K. Tung, and C. P. Yuan, Implications of CTEQ global analysis for collider observables, *Phys. Rev. D* **78**, 013004 (2008).
- [24] L. A. Harland-Lang, A. D. Martin, P. Motylinski, and R. S. Thorne, Parton distributions in the LHC era: MMHT 2014 PDFs, *Eur. Phys. J. C* **75**, 204 (2015).
- [25] J. Butterworth, S. Carrazza, A. Cooper-Sarkar, A. De Roeck, J. Feltesse, S. Forte, J. Gao, S. Glazov, J. Huston, Z. Kassabov *et al.*, PDF4LHC recommendations for LHC Run II, *J. Phys. G* **43**, 023001 (2016).
- [26] S. Bailey, T. Cridge, L. A. Harland-Lang, A. D. Martin, and R. S. Thorne, Parton distributions from LHC, HERA, Tevatron and fixed target data: MSHT20 PDFs, *Eur. Phys. J. C* **81**, 341 (2021).
- [27] A. V. Manohar, P. Nason, G. P. Salam, and G. Zanderighi, The photon content of the proton, *J. High Energy Phys.* **12** (2017) 046.
- [28] A. Szczurek, B. Linek, and M. Łuszczak, Semiexclusive dilepton production in proton-proton collisions with one forward proton measurement at the LHC, *Phys. Rev. D* **104**, 074009 (2021).
- [29] M. Łuszczak, W. Schäfer, and A. Szczurek, Two-photon dilepton production in proton-proton collisions: Two alternative approaches, *Phys. Rev. D* **93**, 074018 (2016).
- [30] E. V. Zhemchugov, S. I. Godunov, E. K. Karkaryan, V. A. Novikov, A. N. Rozanov, and M. I. Vysotsky, libepa – a C++/Python library for calculations of cross sections of ultraperipheral collisions, [arXiv:2311.01353](https://arxiv.org/abs/2311.01353).